https://doi.org/10.5194/egusphere-2023-3082
Preprint. Discussion started: 3 January 2024

Shallow boundary layer heights controlled by the surface-based temperature inversion strength are responsible for trapping home heating emissions near the ground level in Fairbanks, Alaska.

Authors: Meeta Cesler-Maloney[1], William R. Simpson*[1], Jonas Kuhn[2], Jochen Stutz[2], Jennie L. Thomas[3], Tjarda Roberts[4], Deanna Huff[5] and Sol Cooperdock[2]

Affiliations: [1] Geophysical Institute and Department of Chemistry and Biochemistry, University of Alaska Fairbanks, Fairbanks, AK 99775

[2] UCLA Atmospheric & Oceanic Sciences, Los Angeles, CA 90095

[3] Univ. Grenoble Alpes, CNRS, INRAE, IRD, Grenoble INP, IGE, 38000 Grenoble, France

[4] LMD/IPSL, ENS, Université PSL, École Polytechnique, Institut Polytechnique de Paris, Sorbonne Université, CNRS, Paris, France

[5] Alaska Department of Environmental Conservation, P.O. Box 111800, Juneau, 99811-1800

*Corresponding author: William Simpson, wrsimpson@alaska.edu

Abstract

In cold climate cities, like Fairbanks, Alaska, during winter, reduced vertical mixing in the atmosphere leads to pollution trapping and concerningly high $PM_{2.5}$ concentrations at ground level. To study pollution trapping, we simulated dispersion of SO_2 from home heating emissions during the ALPACA-2022 field study in Fairbanks, Alaska using the Platform for Atmospheric Chemistry and Transport one-dimensional model (PACT-1D). Eddy diffusion coefficients that control vertical transport were parameterized by the near-surface temperature inversion strength according

https://doi.org/10.5194/egusphere-2023-3082
Preprint. Discussion started: 3 January 2024

to stable boundary layer (SBL) theory and horizontal export was calculated from the wind speed. The model parameterized the SBL height as a function of the near-surface inversion strength, with the SBL height varying between 50 m for weak inversions down to 20 m for strong inversions. The model results were compared to long-path differential optical absorption spectroscopy (LP-DOAS) concentration profiles and in-situ observations of SO_2 over the range of 3 m to 191 m above downtown Fairbanks over a 33-day period in winter and achieved excellent agreement (R = 0.88). Sensitivity studies showed that the model is most sensitive to the SBL height and the associated eddy diffusivity profile. Model-derived pollution residence times in Fairbanks are on the order of hours during winter, with a median steady state residence time of 2.1 hours under stable atmospheric conditions, indicating there is limited time for chemical processing.

Plain language summary (Short summary)

We used a one-dimensional model to simulate how pollution in Fairbanks, Alaska, accumulates in shallow layers near the ground when temperature inversions are present. We find pollution accumulates in a 20 m to 50 m thick layer. The model agrees with observations of SO_2 pollution using only home heating emissions sources, which shows that ground-based sources dominate sulfur pollution in downtown Fairbanks. Air residence times in downtown are only a few hours, limiting chemical transformations.

Key points

1. The PACT-1D model was used to model pollution in Fairbanks, Alaska, using vertical and horizontal dispersion.
2. Observed path averages of sulfur dioxide measured by LP-DOAS from 12 m to 191 m in downtown Fairbanks for 33 days in winter 2022 were modeled with good skill (R = 0.88).

https://doi.org/10.5194/egusphere-2023-3082
Preprint. Discussion started: 3 January 2024

3. The median pollution residence time was 2.1 hours when the atmosphere was stable, limiting time for chemical processing.

Keywords: one-dimensional modeling, long-path differential optical absorption spectroscopy, vertical profiling, dispersion, Alaska, Fairbanks, pollution trapping, temperature inversion, cold climate

1 Introduction

Weak atmospheric dispersion combined with local emissions sources causes many cold-climate cities to have poor air quality during winter (ALPACA, 2018; Schmale et al., 2018). This poor dispersion is often caused by surface-based temperature inversions, which hinder vertical mixing and prevent winds aloft from penetrating to ground level, where polluted air stagnates. Higher-latitude locations like Fairbanks, Alaska experience frequent surface-based temperature inversions during winter. The Fairbanks North Star Borough is designated by the Environmental Protection Agency (EPA) as a non-attainment area for fine particulate matter, $PM_{2.5}$, which episodically exceeds the 24-hour standard of 35 microgram m^{-3} during winter. While Fairbanks does not exceed the national ambient air quality standards for SO_2, ground level SO_2 mixing ratios can reach 1-hour averages up to 40 nanomole $mole^{-1}$, sometimes for multiple hours (ADEC, 2016). Improvement of air quality in Fairbanks has been a high priority for stakeholders, but our limited understanding of the sources, chemical transformations, and dispersion of pollutants under stagnant winter conditions has hindered these efforts.

Fairbanks residents rely on a variety of fuel sources less commonly used in warmer regions, including wood (both cordwood and pellets) and No. 1 or No. 2 heating oil, both of which have

https://doi.org/10.5194/egusphere-2023-3082
Preprint. Discussion started: 3 January 2024

orders of magnitude higher sulfur content compared to the natural gas and/or ultra-low sulfur diesel (heating oil) that is more widely used in the contiguous USA. Chemical mass balance modeling over a three-winter period from 2008 through 2011 attributed 60% to 80% of $PM_{2.5}$ mass concentration to wood burning in downtown Fairbanks (Ward et al., 2012). A positive matrix factorization analysis by Kotchenruther et al. (2016) attributed 51.8% of $PM_{2.5}$ mass concentration to wood burning in downtown Fairbanks. Recent PMF analysis indicates that the fractional contribution of wood to $PM_{2.5}$ in downtown Fairbanks is trending to smaller amounts in recent years (Ye and Wang, 2020).

Sulfate is the second most prevalent species in $PM_{2.5}$, so understanding sulfur sources and chemistry is important to Fairbanks air quality (Ward et al., 2012). The observed wintertime sulfur oxidation ratio, or the ratio of observed moles of sulfate to total moles of atmospheric sulfur (combined SO_2 and sulfate), is about 5%, which suggests that although secondary chemistry may be adding some sulfate to $PM_{2.5}$, 95% of the sulfur emitted remains in the gas phase as SO_2 (Nattinger, 2016). This low sulfur oxidation ratio is in agreement with recent analysis of sulfate isotopes in Fairbanks during winter, which showed that 62% ±12% of sulfate came from primary sources, with a smaller influence of secondary chemistry (Moon et al., 2024). In addition to home heating sources, vehicles emit CO, $PM_{2.5}$ and NO_x at ground level. Six power plants fueled by coal, diesel, and naphtha, referred to here as point sources, emit large amounts of pollutants. The power plants have tall stacks intended to push their exhaust above the surface-based temperature inversion (ADEC, 2016). While not an air quality regulated pollutant, carbon dioxide (CO_2) is co-emitted by all SO_2 emission sources in Fairbanks and also sourced from mobile sources and other heat sources. Because it does not undergo chemistry and is not consumed by plants in winter, it

https://doi.org/10.5194/egusphere-2023-3082
Preprint. Discussion started: 3 January 2024

can serve as an important marker for combustion processes, as well as the dispersion of these emissions.

While local emissions cause the poor wintertime air quality in Fairbanks, dispersion processes also significantly influence the amount of pollution that accumulates at breathing level. Tran and Mölders (2011) found that $PM_{2.5}$ concentrations in Fairbanks were larger when there were surface-based temperature inversions and stagnant winds near the ground, concurrent with low temperatures, which increase ground level home heating emissions. Surface-based inversions are often intense, with temperature gradients of ~1°C m^{-1} or more observed in the first few meters above the ground level (AGL) on the flat valley floor and can persist throughout the day and even for multiple days during winter (Benson, 1969; Bowling, 1986; Tran and Mölders, 2011; Mayfield et al., 2013; Cesler-Maloney et al., 2022). With the weak vertical dispersion and stagnant horizontal wind speeds near the ground during surface-based inversions, emissions from ground level sources are thought to have a larger impact on ground level pollution in Fairbanks than power plant emissions, although this contribution has only been investigated using numerical models and has not yet been validated by field observations (ADEC, 2016; Tran and Mölders, 2012). This previous work in Fairbanks showed that pollutants were present at higher concentrations during stagnant conditions, indicating that dispersion is crucial to controlling the amount of pollution that accumulates near ground level.

There are two distinct mechanisms responsible for the development of surface-based temperature inversions in Arctic regions: radiative cooling at the surface and warm air advection (Busch et al., 1982; Bowling, 1986; Bradley et al., 1992; Bourne et al., 2010; Zhang et al., 2011). During radiative cooling, heat is lost by infrared radiation from the ground, and air near the ground that interacts with this cooling surface decreases in temperature more than the air at higher

https://doi.org/10.5194/egusphere-2023-3082
Preprint. Discussion started: 3 January 2024

altitudes. These radiative cooling inversions become more intense on nights with clear sky conditions. The formation of surface-based inversions during winter in Fairbanks is also supported by the high emissivity of snow in the thermal infrared and the high albedo of snow in the visible, limiting solar heating. When the warm air advection mechanism occurs, warmer, more buoyant, air masses are advected over colder, denser, air masses laying near the surface, creating a surface-based temperature inversion.

During surface-based inversions, the atmosphere is stable with regard to buoyancy, which reduces turbulence, but mechanical friction of wind acting on the surface roughness leads to some mixing. This stable part of the atmosphere located near the ground level during surface-based inversions is referred to as the stable boundary layer (SBL). On short time and length scales, this mixing is highly complex, including intermittency and often showing oscillations (Mahrt, 1981); however, simpler 1-D empirical theories are able to describe effective turbulent transport in the SBL with good agreement to observations on longer timescales or via spatial averaging. Monin-Obukhov similarity theory defines a set of functions to describe the vertical mean flow and temperature in the surface layer as a function of dimensionless height, which is related to actual height using the Obukhov length parameter, L_{MO} (Monin and Obukhov, 1954; Mahrt, 1989). The Obukhov length is a key parameter in many of these turbulence models, along with the SBL height, h, which is the height above which the atmosphere is no longer influenced by contact with the surface. Vertically mixing turbulent eddies exist between the ground surface and the top of this SBL, but there is little vertical exchange in the free troposphere above the SBL height. Past work has shown that the SBL height decreases with increased surface cooling rate, sometimes to SBL height of just tens of meters (Mahrt, 1981; Wyngaard, 1975; Brost and Wyngaard, 1978; Stull, 1983; Nieuwstadt, 1984a, b).

https://doi.org/10.5194/egusphere-2023-3082
Preprint. Discussion started: 3 January 2024

Empirical theories that describe bulk turbulence in the SBL parameterize vertical mixing through the eddy diffusivity coefficient for momentum (K_z) (Newsom and Banta, 2003; Nieuwstadt, 1984b; Wyngaard, 1975; Brost and Wyngaard, 1978; Beare et al., 2006; Degrazia and Moraes, 1992). These models have a K_z vertical profile that peaks at an altitude that is roughly 20% of the SBL height and decreases to the molecular diffusion limit (near zero) both at the surface and above the top of the SBL (Kuhn et al., 1977; Nieuwstadt, 1984a; Brost and Wyngaard, 1978; Degrazia and Moraes, 1992; Beare et al., 2006). In this work, we will use these models for the K_z vertical profile to describe vertical mixing within the SBL.

Here, the Platform for Atmospheric Chemistry and Transport one-dimensional (PACT-1D) atmospheric column model (Tuite et al., 2021; Ahmed et al., 2022) was used to analyze how the dispersion of pollution depends on meteorological conditions during winter in Fairbanks. The model simulates vertical turbulent mixing with high vertical resolution and uses horizontal exchange with the unpolluted ambient atmosphere driven by winds to simulate dispersion of SO_2 emissions in downtown Fairbanks. Model results were validated against path-averaged field observations of SO_2 measured by a long-path differential optical absorption spectroscopy (LP-DOAS) instrument deployed in downtown Fairbanks as part of the Alaskan Layered Pollution And Chemical Analysis (ALPACA) study, which was carried out in Fairbanks during January and February 2022 (Simpson et al., submitted 2023). Model results were also compared with in-situ SO_2 observations at 3 m AGL and CO_2 measurements at 3 m and 23 m AGL. PACT-1D simulations were also used to calculate the transport loss rates of pollution from both vertical and horizontal dispersion to understand the residence time of pollution in the urbanized area of Fairbanks. Having an estimate of the residence time of pollution in the city helps to provide a constraint on the timescales for chemical processing in Fairbanks. With a better understanding of these dispersion

https://doi.org/10.5194/egusphere-2023-3082
Preprint. Discussion started: 3 January 2024

processes, communities and regulatory agencies can better predict the timing and severity of pollution events and develop improved strategies for pollution mitigation based on meteorological forecasts.

2 Field measurements from the ALPACA campaign

The ALPACA field campaign took place at multiple sites in Fairbanks in winter, from January 17 to February 25, 2022. Fairbanks, located in central Alaska near the Arctic circle, is one of the few urbanized cities in the region and lies within a basin, surrounded by hills to the north, east and west, with flat lands to the south. Fairbanks winters are characterized by short daylight hours and extremely cold temperatures with frequent surface-based inversions.

Measurements used in this manuscript were made in downtown Fairbanks at two sites: the University of Alaska Fairbanks Community and Technical College field site (CTC site, 64.841°N, –147.727°E) and at the LP-DOAS base at 17 m AGL on the top floor of the Lacey-Street Parking Garage (64.844°N, –147.716°E), which lies 610 m east-northeast of the CTC site. Figure 1 shows a map of the relevant ALPACA measurement locations in Fairbanks. The nine boxes shown in Figure 1 are the Weather Research Forecast / Community Multiscale Air Quality model (WRF/CMAQ) 1.33 km-scale grid cells that were co-added to be the emissions footprint of PACT-1D, as described in Section 3. The emissions inventory and WRF/CMAQ model was developed by the U.S. Environmental Protection Agency (EPA) and the Alaska Department of Environmental Conservation (ADEC). The LP-DOAS measured path-averaged trace gas mixing ratios across four slightly inclined paths viewing north-east towards Birch Hill, a ~200 m tall hill. The shortest path was ~1 km to the north-east from the base to a retroreflector situated at 12 m AGL on the Nordale Elementary School building. The other three paths were roughly 4 km long and had retroreflectors

https://doi.org/10.5194/egusphere-2023-3082
Preprint. Discussion started: 3 January 2024

at altitudes of 73 m, 115 m and 191 m AGL at the LP-DOAS base. Nearly all of the populated portion along these paths was within a few meters above the flat valley floor. The LP-DOAS instrumentation used in the ALPACA field campaign is similar to the instrumentation used in past studies to measure vertical profiles of UV-absorbing trace gases in urban environments and uses analytical methods described in Platt and Stutz (2008) (Stutz et al., 2004; Tsai et al., 2014).

Temperature was measured at 3 m, 6 m, 11 m and 23 m AGL using aspirated thermometers (Cesler-Maloney et al., 2022). The 3 m, 6 m and 11 m temperature probes were deployed on the tower of a small stationary trailer in the parking lot of the CTC site, while the 23 m temperature probe was deployed above the elevator shaft house roof on top of the CTC building. An RM Young 1005 wind speed and direction monitor was co-located with the 23 m temperature sensor. The relative precision of these temperature sensors was better than 0.15 °C over the range from 20 °C to −60 °C (Cesler-Maloney et al., 2022).

In-situ SO_2 (Thermo Scientific 43C) was measured from an inlet at 3 m AGL in a larger stationary trailer parked next to the CTC building. The SO_2 analyzer was calibrated using an EPA certified mixed standard containing 5.190 micromole mole^{-1} SO_2 and 508.4 micromole mole^{-1} CO by overflowing the inlet with zero air or standard gas diluted in zero air at multiple calibration mixing ratios using an Environics 9100 calibration dilution system. The gas analyzer was calibrated roughly weekly and this multi-point calibration slope and zero were applied to the data by linearly interpolating them in time between calibrations. Two Vaisala (GMP343) CO_2 instruments were also deployed at the CTC site, one at 3 m AGL on the small trailer and the other at 23 m AGL on the roof of the CTC building. The CO_2 instruments were co-located at the same altitude on the small trailer both before and after the field campaign and the older instrument was corrected to the newer instrument that had a recent factory calibration within the prior year. Trace

https://doi.org/10.5194/egusphere-2023-3082
Preprint. Discussion started: 3 January 2024

gases (O_3, carbon monoxide (CO) and NO_x) were also measured at the CTC site and O_3 was measured by a second instrument at 158 m AGL on Birch Hill (see the Supplemental Materials for more information).

3 Methods

3.1 Description of the PACT-1D model

One-dimensional (1-D) chemical transport models simulate coupled dispersion and chemical processes to predict the vertical profiles of pollutants. These 1-D models have simulated vertical profiles of trace gases in urban areas, such as Houston, Texas and Los Angeles, California, with good agreement to observations (Geyer and Stutz, 2004; Stutz et al., 2004; Tsai et al., 2014; Tuite et al., 2021). Vertical and horizontal transport processes can both be simulated within the 1-D model's column. Horizontal transport can be considered as an entrainment of background air from outside of a polluted region into the modeled column layers. Fairbanks, being a small city encircled by the sparsely populated boreal forest, is well suited for 1-D modeling with added horizontal dilution by surrounding background air. This horizontal transport process is implemented in the model by adding a pollution exchange term proportional to the windspeed divided by the length scale of the urban area (see Section 3.3).

Here, we use a vertical grid, which divides the lower atmosphere (up to 1000 m AGL) into 39 vertical layers that vary in thickness, being denser near the ground. The PACT-1D model simulates vertical exchange through eddy flux-gradient formalism, using vertical eddy diffusion coefficients, K_z, for each layer.

The PACT-1D model was used in a dispersion-only mode, without simulating chemical processes and SO_2 is used as a dispersion tracer of Fairbanks pollution. We chose SO_2 because it

https://doi.org/10.5194/egusphere-2023-3082
Preprint. Discussion started: 3 January 2024

has a well quantified and spatially distributed ground level source from home heating oil combustion and its vertical distribution was measured by LP-DOAS during ALPACA, which is used to validate the model results. Although SO_2 can be lost via chemical oxidation, the observed sulfur oxidation ratio during Fairbanks winter is small, with only 5% of the total atmospheric sulfur appearing as sulfate in observations (Nattinger, 2016). In addition to SO_2, CO_2 was also modeled as a passive tracer of dispersion and validated against in-situ observations of CO_2 from the CTC building site in Figure 1.

3.2 Treatment of vertical exchange

It is difficult to model vertical exchange in the shallow SBL, so we used a simple model from literature to determine the vertical profile for K_z. Input K_z profiles for PACT-1D were calculated under SBL conditions using Equation EQ1 from Brost and Wyngaard (1978), where h is the SBL height, z is the altitude and L_{MO} is the Monin-Obukhov length.

$$K_z(z) = \kappa u^* h \frac{(z/h)(1-z/h)^{1.5}}{1+4.7(z/h)(h/L_{MO})} \quad \textbf{EQ1}$$

In Equation EQ1, constant values were used for the von Kármán constant, κ = 0.4, the friction velocity, u^* = 0.40 m s^{-1}, and the ratio of h/L_{MO} = 1.4. Brost and Wyngaard showed that variations in h/L_{MO} had only small effects on the vertical shape and peak of the K_z profiles calculated by Equation EQ1.

With these assumptions, the K_z profile only depends upon the SBL height, h. For simulation of the ALPACA field campaign period, the SBL height was parameterized as a function of the near-surface atmospheric stability, which we quantify using the 23 m minus 3 m temperature difference at the CTC site, $dT_{[23m-3m]}$. When $dT_{[23m-3m]}$ is large and positive, the atmosphere is very stable, and when it is near zero or slightly negative, the atmosphere is neutral. Past work

https://doi.org/10.5194/egusphere-2023-3082
Preprint. Discussion started: 3 January 2024

253 demonstrates that when stability is very strong, the SBL height is shallow (Mahrt, 1981;
254 Wyngaard, 1975; Brost and Wyngaard, 1978; Stull, 1983; Nieuwstadt, 1984a, b). Conversely, as
255 $dT_{[23m-3m]}$ approaches neutral conditions (near zero), the SBL height is expected to increase. Based
256 upon this relationship between $dT_{[23m-3m]}$ and stability, a lookup table was created to calculate h
257 from $dT_{[23m-3m]}$, which was linearly interpolated between nodes in Table 1. Section 5.2 will discuss
258 the relationship between the SBL height, h, and the surface-based temperature inversion strength,
259 $dT_{[23m-3m]}$ in Table 1 in more detail.

260 Sensitivity studies were used to determine how model results depend upon these
261 parameterized SBL heights. When the atmosphere was near neutral ($dT_{[23m-3m]} < 0.2$ °C), Equation
262 EQ1 was used with a value $h_{neutral} = 400$ m, representing a tall SBL height. Figure S2 in the
263 Supplemental Materials shows that the resulting K_z profile in the critical near-surface region is
264 nearly the same whether $h_{neutral} = 400$ m, a larger SBL height or even a neutral K_z profile is chosen.
265 Sensitivity studies will test the model result's dependence on this choice of a near-neutral SBL
266 height.

267

268

269 **3.3 Treatment of horizontal exchange**

270 The PACT-1D model was used in the configuration described in Tuite et al. (2021), but
271 with an added horizontal dispersion term, as described in Equation EQ2.

272 $$K_{EXCH} = v \,/\, L \qquad \textbf{EQ2}$$

273 Equation EQ2 represents the standard mass-balance approach result for the dependence of the
274 horizontal exchange coefficient, K_{EXCH}, on wind speed, v, and the length of Fairbanks, L (Jacob,
275 1999). Here, a horizontal characteristic length scale of $L = 4$ km is the length of the footprint of

https://doi.org/10.5194/egusphere-2023-3082
Preprint. Discussion started: 3 January 2024

the model column and was meant to represent the urban core of Fairbanks (Figure 1). The wind speed at each model layer altitude is used to calculate a layer-specific exchange rate. Sensitivity studies are used to test the model's response to varying this horizontal length parameter.

Constant wind speed profiles were used in idealized (steady state) model simulations, while a combination of WRF-modeled and observed wind speeds were used as model inputs in simulations of observed pollution events. Wind speeds from the WRF model were provided by the U.S. EPA, which was sampled at the middle of the modeled area at 64.842°N, -147.700°E. Observed wind speeds were measured at 23 m at the CTC site and also at 2 m and 10 m at the nearby ADEC NCore site, located roughly 500 m north of the CTC site (Figure 1). When observed winds were used as model inputs, the wind speed was linearly interpolated between 2 m (NCore), 10 m (NCore), 23 m (CTC) and 50 m (WRF) and only WRF winds were used above 50 m AGL. The WRF wind speeds were compared to radiosonde data from the Fairbanks Airport and were found to be in good agreement to radiosonde wind speeds in the first 500 m AGL.

3.4 Treatment of emissions

Emissions for Fairbanks were provided by the ADEC as hourly total emissions for the sum of nine WRF/CMAQ (1.33 km resolution) grid cells arranged in a 3x3 grid cell = 4 km x 4 km = 16 km^2 area in downtown Fairbanks. This emissions area has a bounding box with NW corner: 64.861°N, -147.743°E and SE corner = 64.824°N, -147.658°E and includes the NCore site, the CTC site, the A-Street site, the LP-DOAS base station and nearly all of the LP-DOAS paths up Birch Hill, as shown in Figure 1. Downtown emissions rates were converted to moles m^{-2} s^{-1} using

https://doi.org/10.5194/egusphere-2023-3082
Preprint. Discussion started: 3 January 2024

the footprint of this emission area. Because PACT-1D has no horizontal dimensions, emissions sources are instantaneously mixed throughout the layer in which they are emitted, such that the model would not be able to capture the horizontal variability in emissions if sources were not homogenously distributed across the area being modeled. However, SO_2 is emitted from hundreds of homes within the 16 km^2 area in downtown Fairbanks, providing a distributed source that may make the model's assumption of horizontal mixing within the column be more realistic.

The main source of SO_2 emissions near ground level is from home heating, as most homes in Fairbanks relied on sulfur-rich No. 2 or No. 1 heating oils at the time of the ALPACA field campaign, thus only home heating emissions data was used in model simulations. Pollutant emissions from home heating sources were distributed into PACT-1D by altitude, with 40% in the PACT-1D layer from 3 m to 6 m, 50% in the PACT-1D layer from 6 m to 9 m and 10% PACT-1D layer from 9 m to 12 m. Carbon dioxide (CO_2) is produced in many combustion processes, allowing CO_2 to be used as a tracer for anthropogenic pollution in the atmosphere. The ADEC does not report CO_2 emissions, so an empirical emissions ratio of CO_2 to SO_2 was used to determine the emissions rate for CO_2 in the model. A linear fit for observed 3 m CO_2 versus SO_2 at CTC was calculated, where the intercept is interpreted to be the CO_2 background mixing ratio surrounding Fairbanks (420 micromole $mole^{-1}$) and the slope is the empirical emissions ratio of 4300 moles CO_2 to 1 mole SO_2, such that multiplying the SO_2 emissions ratio by this slope yields the CO_2 emissions rate in the model (see Supplemental Materials Figure S1).

3.5 Diagnosing vertical and horizontal exchange

To diagnose the transport rate of SO_2 by vertical and horizontal dispersion in PACT-1D, two loss rates were determined; the vertical loss rate out of the "urban canopy", defined as the

https://doi.org/10.5194/egusphere-2023-3082
Preprint. Discussion started: 3 January 2024

layer from zero to 15 m AGL (approximate height of trees and buildings) and denoted as L_{canopy}, and the vertically integrated horizontal loss rate across the model column, denoted as L_{export}. The PACT-1D model calculates vertical transport exchange rates for each layer (denoted VT_{layer}), where positive rates represent net gain of concentration of a species in that layer by vertical transport from neighboring layers and negative rates a net concentration loss. Equations EQ3 and EQ4 show the transport loss rates calculated from model output.

$$L_{canopy} = \sum_{layers\ 0m-15m}(-VT_{layer} \times layer\ height) \quad \textbf{EQ3}$$

$$L_{export} = \sum_{all\ layers}\left(K_{exch\_layer} \times layer\ height \times \left([C]_{layer} - [C]_{bg}\right)\right) \quad \textbf{EQ4}$$

In this equation, $[C]$ represents the concentration of a species in each layer or in the background air that replaces horizontally exported air. Both loss rates have units of column density per time, mole m^{-2} s^{-1}. Because the considered sources emit only within the urban canopy layer and background air is cleaner than the polluted column being considered, both rates are positive, indicating vertical transport upwards, out of the urban canopy, and export of pollution horizontally out of the considered polluted urban column.

3.6 Diagnosing steady state residence times for vertical and horizontal loss processes

The steady-state lifetime of a box model is defined by Jacob (1999) as the ratio of the amount of any species in the box divided by the total loss rate for that species out of the box. As chemistry was not considered in this application, we refer to our box-model lifetime outputs as "residence times" to clarify that we are only considering losses from transport processes. Two steady-state residence times were defined here to analyze atmospheric dispersion processes, the urban canopy column residence time (τ_{canopy}), which is the column density of a species in the urban

https://doi.org/10.5194/egusphere-2023-3082
Preprint. Discussion started: 3 January 2024

canopy (i.e., the concentration integrated vertically from the ground to the urban canopy height) divided by L_{canopy} and the column export residence time (τ_{export}) which is the downtown column density of a species (i.e., the concentration integrated vertically from the ground to the top of the model column) divided by the column export loss rate, L_{export}. When the model simulates idealized cases and is run until steady state is achieved, these residence times are completely accurate. For the model simulations of observed SO_2 during the ALPACA campaign, sources and sinks vary with time such that the system is not at a true steady state. However, we assume it is "near steady state" for the purposes of calculation of residence times, and as we will demonstrate, residence times are short indicating that the system approaches steady state on similarly short timescales.

4 Results

4.1 Conceptual model for pollution trapping in Fairbanks

Figure 2 shows a conceptual model of the horizontal and vertical dispersion processes in Fairbanks and was used to inform the setup of the PACT-1D simulations for Fairbanks. In Figure 2, the horizontal arrows representing wind show that there is little to no wind present near ground level and wind increases with altitude, staying relatively slow in the urban canopy (due to friction on ground roughness) and increasing to the top of the SBL. The vertical arrows in Figure 2 represent vertical transport based on the SBL parameterization described in the introduction, where vertical exchange between layers increases from near zero at the ground level to a maximum at roughly 20% of the SBL height, then decreases to near zero above the SBL.

A series of idealized model simulations with simplified boundary conditions that were constant in time (*i.e.*, *h,* wind speed profile, emissions) were performed to observe approach to steady state and verify model closure. These idealized model simulations based on the conceptual

https://doi.org/10.5194/egusphere-2023-3082
Preprint. Discussion started: 3 January 2024

model in Figure 2 enable a validation and a more intuitive understanding of the model scheme. Figure 3 shows results from simulations that used a constant emission rate, time-invariant vertical profile of wind speed and constant SBL height, h, as shown in Table 2. The SO_2 emissions rate is $6x10^{-9}$ moles m^{-2} s^{-1} SO_2, similar to the average wintertime SO_2 emissions in Fairbanks.

The case 1 simulation (h = 25 m, 2 m s^{-1} wind above SBL) achieves a 3 m AGL steady state SO_2 mixing ratio of ~35 nanomole $mole^{-1}$ in about four hours (Figure 4). When the input SBL height is doubled from 25 m in case 1 to 50 m in case 2, the peak value of K_z roughly doubles, accelerating vertical export from the urban canopy. The result of this doubling of the SBL height is to cut the steady state urban canopy SO_2 mixing ratio roughly in half. When the wind speed aloft is changed from 2 m s^{-1} to 5 m s^{-1} without changing the SBL height in case 2 and case 3, the steady state SO_2 mixing ratio decreases further because there is a greater horizontal export in the polluted layers from 15 m to 50 m. In the case 1 and case 2 simulations with a constant wind speed of 2 m s^{-1} aloft and an input SBL height $h \lesssim 50$ m, the height of the polluted layer is nearly the input SBL height, yielding a sigmoid shaped profile (see Figure 3). In contrast, case 3 shows that higher winds aloft remove pollution in upper layers more effectively and yields a more triangular shape with the effective height of the polluted layer is somewhat shorter than the input SBL height, h. Case 4 shows that for a taller SBL height (100 m), even with low winds, the simulation gives a triangular vertical profile.

Figure 4 shows a false-color plot of the vertical profiles of SO_2 over a 12-hour simulation for case 2 (top panel) and the ratio of the vertical loss rate out of the urban canopy, L_{canopy}, and the downtown column horizontal export loss rate, L_{export}, to the constant emissions rate for SO_2, showing that the model achieves a steady state in about four hours, where SO_2 accumulates in the surface layer until the emissions and the loss rate out of the SBL balance each other. Note that the

https://doi.org/10.5194/egusphere-2023-3082
Preprint. Discussion started: 3 January 2024

vertical exchange precedes the horizontal export because vertical transport into the windy region from 15 to 50 m is required for pollution export. As expected, when steady state is achieved, the horizontal export loss rate from the model and the upward loss rate from the urban canopy are both equal to the emission rate. This simulation demonstrates that for realistic conditions in Fairbanks, near steady state is achieved in a few hours, which indicates that use of the steady state residence time to diagnose time-varying simulations is reasonable.

4.2 Observations and modeling for the ALPACA campaign

Figure 5, panels A through E, show time series of different measurements during the ALPACA field campaign from January 15 to February 28, 2022. There were multiple times during the ALPACA campaign that had low temperatures (panel A), persistent temperature inversions, as indicated by a positive 23 m minus 3 m temperature differences ($dT_{[23m-3m]} > 0$) (panel B), small wind speeds on the 23 m vertical scale (panel C), differences in CO_2 on the 23 m vertical scale (panel D, with more CO_2 at 3 m than at 23 m) and accumulation of SO_2 at ground level (panel E). During the persistent temperature inversion event that occurred during the "cold-polluted period" (January 30th through February 4nd), CO_2 reached a relatively constant mixing ratio at 3 m AGL by around midnight on January 31st and maintained similar levels until SBL breakup by winds from aloft on February 4th.

With ongoing emissions throughout the persistent inversion event, this near-steady pollution behavior can only be explained by a pollution export from the SBL, as in the conceptual model shown in Figure 2. At times when the SBL is above the higher altitude (23 m AGL), CO_2 reaches equivalent mixing ratios at both 3 m and 23 m AGL and conversely when the SBL is near or below the top CO_2 sensor, mixing ratios are larger at 3 m and smaller at 23 m AGL. There are

https://doi.org/10.5194/egusphere-2023-3082
Preprint. Discussion started: 3 January 2024

even periods (e.g., on February 3rd) when CO_2 at the 23 m altitude is near the regional background of ~420 micromole $mole^{-1}$, indicating it is above the SBL, in the free troposphere and that the SBL height must be below 23 m.

Figure 6 panels A and B show false-color time series of the model output SO_2 mixing ratio and wind speed profiles, respectively. The model was not sensitive to changes in the time step for dispersion processes, as there was no change in the slopes and *R* values for either SO_2 or CO_2 when the time step in the model (typically 5 seconds) was doubled to 10 seconds or decreased to 2.5 seconds. Figure 6 also shows a time series of the downtown column emissions in panel C and model input SBL height in panel D. When the SBL height is small, pollution is trapped in a similarly short and increasingly concentrated layer in Figure 6. At times when the SBL is near neutral (off scale vertically in panel D), pollution mixing ratios were small throughout the vertical column, as would be expected for fast vertical mixing and dilution implied by a tall SBL height. The modeled concentration profile time series shown in Figure 6 panel A can be integrated vertically between the LP-DOAS base altitude (17 m) and the height of the retroreflector on that LP-DOAS path to give the model-predicted path-averaged SO_2 mixing ratio for that path. Therefore, the four LP-DOAS paths, here denoted as P0 to P3 represent the average mixing ratio from 17 m to 12 m, 73 m, 115 m, and 191 m AGL at the LP-DOAS base, respectively.

Figure 7 panels A through D show time series plots of the hourly path-averaged SO_2 from PACT-1D, LP-DOAS field observations, and in-situ 3 m field observations (panel A only). In Figure 7 panel A, the model path 0 (P0, 12 m to 17 m AGL) averaged SO_2, the LP-DOAS path 0 average SO_2 and the in-situ 3 m SO_2 all show good agreement in the time series, with mixing ratios of 20 to 40 nanomole $mole^{-1}$ observed in the urban canopy layer when polluted. The trapping of SO_2 near ground level in Figure 7 panel A occurs at times with surface-based temperature

https://doi.org/10.5194/egusphere-2023-3082
Preprint. Discussion started: 3 January 2024

inversions (low SBL height) and slow wind speeds within the urban canopy layer. In Figure 7 panel B, the timing of SO_2 peaks observed by the LP-DOAS on path 1 (P1, 17 m to 73 m AGL) matches the peaks observed on path 0, in panel A, however the magnitude of SO_2 pollution is smaller, only reaching up to 15 nanomole $mole^{-1}$ in panel B. In Figure 7 panels C and D, the magnitude of SO_2 pollution observed continues to decrease with altitude and there are also some SO_2 peaks observed by the LP-DOAS on paths 2 (P2, 17 m to 115 m AGL) and 3 (P3, 17 m to 191 m AGL) that are not present in the path-averages modeled by PACT-1D, particularly during the persistent surface-based temperature inversion event during the "cold-polluted period" in Figure 5. We hypothesize that these peaks on paths 2 and 3 are due to elevated power plant emission plumes that are horizontally transported into the upper light paths. However, this 1-D model is not suited for simulations of power plant emission dispersion, an inherently 3-D, process, so later 3-D modeling would be required to analyze these infrequent spikes in the upper two LP-DOAS path data.

4.3 Correlation of modeled pollution to observations

Figure 8 shows four modeled versus observed SO_2 correlation plots of data averaged at 3-hour time resolution, which was used to diagnose the skill of the model in simulating observed SO_2 mixing ratios. Linear fits are shown with either a constrained zero intercept or a free intercept. Figure 8 panel A represents the overall agreement between LP-DOAS and model path-averages across all paths, panel B represents the agreement of the model to in-situ SO_2 observations at 3 m AGL and panels C and D represent the agreement between the model and LP-DOAS path-averages in the first two paths (path 0 and path 1, respectively), which are the paths where a majority of the

https://doi.org/10.5194/egusphere-2023-3082
Preprint. Discussion started: 3 January 2024

pollution observed by the LP-DOAS is located. Correlation plots of the modeled path 2 and path 3 SO_2 versus the LP-DOAS are shown in Figure S3 in the Supplemental Materials. The PACT-1D model showed good agreement with observations, as the *R* values for all DOAS path-averaged data (Figure 8 panel A) and in the urban canopy (Figure 8 panels B and C) are all greater than 0.8. The observed and modeled SO_2 mixing ratios on the upper two paths are usually small and the correlation in Figure 8 panel A is dominated by data from path 0 and path 1. Figure 7 panel A shows that the path-averaged path 0 SO_2 observed by the LP-DOAS has good agreement with the in-situ SO_2 observed at 3 m AGL, with a zero-intercept linear correlation *slope* = 0.95 and *R* = 0.89 (see Figure S4), suggesting that SO_2 is well mixed within the ~15 m AGL urban canopy layer.

Figure 9 shows a time series of hourly averaged model and in-situ CO_2 at 23 m (middle panel) and at 3 m (bottom panel) and the modeled and observed 23 m minus 3 m CO_2 difference, $dCO_{2[23m-3m]}$. The model simulated observed CO_2 with good agreement, with a 3-hour average free-intercept *slope* = 0.75 and *R* = 0.83 for the 3 m CO_2 data and a *slope* = 0.73 and *R* = 0.74 for the 23 m CO_2 data (see Supplemental Materials Figure S5). The top panel of Figure 9 shows that while the model does capture the timing of pollution trapping in the first 23 m, there are still many times when the model overestimates CO_2 at 23 m.

4.4 Model residence times during ALPACA

For the duration of the ALPACA field campaign, the urban canopy residence times (τ_{canopy}) and column export residence times (τ_{export}) for SO_2 were calculated from PACT-1D model outputs (see Supplemental Materials Figure S6). Figure 10 shows the log-time distribution of the urban canopy (left panel) and column export (right panel) SO_2 residence times. The urban canopy residence times in the left panel of Figure 10 have a bimodal distribution, where the mode with

https://doi.org/10.5194/egusphere-2023-3082
Preprint. Discussion started: 3 January 2024

shorter residence times from 0.1 hours (6 minutes) to around 0.33 hours (20 minutes) occur during near-neutral surface atmospheric stability conditions and the mode with longer residence times from around 0.33 hours (20 minutes) to 2.4 hours occurs during stable atmospheric conditions.

During stable conditions with an SBL height, $h \lesssim 50$ m, data in the left panel of Figure 10 has a log-normal distribution with a median $\tau_{canopy} = 54$ minutes. The median urban canopy residence time of the data overall was $\tau_{canopy} = 40$ minutes. The histogram in the right panel of Figure 10 has log-normal distribution has overlapping modes indicating that the column export residence time is less affected by changes in atmospheric stability, with a median $\tau_{export} = 1.8$ hours overall and $\tau_{export} = 2.1$ hours during stable conditions. In Figure 11, the urban canopy and column export SO_2 residence times are plotted against the modeled SBL height from Table 1. The urban canopy residence time in the top panel in Figure 11 is anti-correlated with SBL height, increasing with decreasing SBL height. Some of the column export residence time data in the bottom panel in Figure 11 is anti-correlated with SBL height, but there is more spread in the data as short residence times are sometimes observed at times with shallow SBL heights.

5 Discussion

5.1 Relationship between steady state vertical profile shape and SBL height

Figure 3 shows that the shape of the SO_2 vertical profile depends upon the SBL height and wind profile. For shallow SBL heights and low winds aloft, the model simulates a sigmoidal shape with the polluted layer extending to the SBL height, while for taller SBL height and higher winds aloft, the SO_2 profile becomes a more triangular shape and the effective pollution layer height is below the SBL height, as observed when comparing the Figure 3 cases 3 and 4 simulation to the case 1 and case 2 simulations. This shows that the SBL height is a critical parameter for simulating

https://doi.org/10.5194/egusphere-2023-3082
Preprint. Discussion started: 3 January 2024

the vertical distribution of pollution in Fairbanks, but also that the wind speed aloft affects the shape.

The conceptual model presented in Figure 2 assumed there is an urban canopy from zero to 15 m AGL where wind speed is low. This canopy has roughness elements, buildings and trees, throughout it, which convert small winds into turbulence, enhancing mixing in this layer, while slowing horizontal wind speed. The observations demonstrate that this layer is mechanically mixed because the LP-DOAS path 0 average (average measurement height of 15 m) was well-correlated with the in-situ SO_2 measured at 3 m at the CTC site (zero-intercept *slope* = 0.95 and R = 0.89). At times when the winds have effectively stagnated in the urban canopy layer, export of pollution occurs by upward transport from the urban canopy to windier layers aloft, as shown in the idealized simulation represented in Figure 4 and vertical canopy flux approaches the source flux before winds aloft can export this pollution, as represented by the export flux. In this idealized situation, steady state is achieved in a few hours.

5.2 Relationship between pollution trapping and temperature inversion strength

In Table 1, the SBL height decreases with increasing surface-based inversion strength and does not exceed 50 m AGL unless the inversion weakens enough to allow the SBL to be near neutral. When the atmosphere is near neutral, a large value of h = 400 m is used to allow larger amounts of vertical transport to occur in the boundary layer, which leads to the dilution of pollution in the model column representing downtown Fairbanks. This process is responsible for the rapid cleanout events that occur episodically throughout the winter (*e.g.*, see Figure 5).

https://doi.org/10.5194/egusphere-2023-3082
Preprint. Discussion started: 3 January 2024

At times when the SBL height is very shallow, CO_2 accumulates to large mixing ratios near ground level and vertical differences in CO_2 are seen across the CTC building in Figure 6, as vertical transport is limited to a shallow vertical extent within the SBL and winds above the SBL can quickly dilute pollution to background mixing ratios aloft. There are few of these periods with extremely large $dT_{[23m-3m]}$, such as the end of the "cold-polluted period" (February 3rd) and the "warm-polluted period" at the end of ALPACA from February 23rd through 25th, and late on January 23rd. During these times, the CO_2 sensor at 23 m AGL was nearly at regional background CO_2, about 420 micromole $mole^{-1}$, as would be expected if it were in the free troposphere, above the SBL height. These observations help to verify that the urban canopy in downtown Fairbanks can be below 23 m at times when $dT_{[23m-3m]}$ is very large, as was used in the parameterization of h versus $dT_{[23m-3m]}$ in Table 1. Past work also demonstrated significant trapping of $PM_{2.5}$ on the 20 m vertical scale under strongly stable conditions in Fairbanks, further motivating the minimum value of h used in Table 1 (Cesler-Maloney et al., 2022).

When choosing the maximum SBL height in Table 1, we knew this height must exceed 23 m during weaker surface-based inversions, as there were times when CO_2 mixing ratios were more equivalent at 3 m and 23 m during inversions in Figure 6. In Figure 7, the path averaged mixing ratios of SO_2 during surface-based temperature inversions were largest in path 0 from 12 m to 17 m, reaching a maximum of ~40 nanomole mol^{-1}, and were smaller in path 1 from 17 m to 73 m, reaching a maximum of ~15 nanomole mol^{-1}. These SO_2 observations show that during inversions, the SBL height is greater than 17 m but doesn't reach 73 m, as there must be cleaner air somewhere in path 1 to make the path averaged SO_2 mixing ratio less than what is observed in path 0. Therefore, we chose a maximum SBL height of 50 m during weak surface-based inversion conditions in Table 1. Between the very strong inversion the weak inversion cases, we mapped out

https://doi.org/10.5194/egusphere-2023-3082
Preprint. Discussion started: 3 January 2024

an inverse curve that was then interpolated to give the SBL height from the near-surface inversion temperature difference. These choices of SBL heights in Table 1 were informed by observations and proved to model observations with excellent agreement. Sensitivity studies were also carried out and discussed in Section 5.4 to examine the result of choosing higher or lower values of the SBL height, h.

5.3 Skill of PACT-1D in modeling observed SO_2 vertical profiles

The modeled SO_2 path averaged and 3 m SO_2 mixing ratios have excellent agreement with observations when PACT-1D simulated the full ALPACA campaign period, as indicated by the R values of 0.88 and 0.81 in Figure 8 panels A and B, respectively. The home heating emissions and the wind speeds used to calculate the horizontal exchange coefficient representative of Fairbanks based on the best available data from ADEC and EPA. The overlap between the SBL height and the vertical wind speed profile is the most important factor controlling pollution trapping in Fairbanks. When the SBL height is large enough, emissions are mixed more quickly through a taller section of the vertical column, where they intersect with altitudes having larger horizontal exchange. This vertical ventilation results in a more well-mixed column with small mixing ratios of SO_2 at ground level, as observed both in the model and in the DOAS data at times when the SBL is near neutral ($h > 50$ m) in Figure 6.

5.4 Model sensitivity studies

To explore the sensitivity of model results to input parameters, a series of simulations were carried out, as described in Table 2, which varied parameters from the "Base" simulation described above. The zero-intercept linear correlation slopes and R values for the "Base" simulation and each

https://doi.org/10.5194/egusphere-2023-3082
Preprint. Discussion started: 3 January 2024

sensitivity study are reported in Table 3. The y-intercepts for free-intercept fits are shown in Supplemental Materials, Table S1 and are typically just a few nanomole $mole^{-1}$. The path 1 to path 0 slope ratio (Table 3) was the metric used to gauge the model's success in simulating the observed vertical shape of SO_2 above Fairbanks. In Table 3, decreasing the SBL height decreased the slope ratio from the "Base" 1.00 to 0.59, while increasing the SBL height increased the P1/P0 slope ratio to 1.47, showing that the SO_2 vertical gradients are highly sensitive to changes in SBL height. Therefore, we find that the model parameterization's very shallow SBL heights, h = 20 to 50 m are required for a realistic simulation of the vertical shape of the polluted layer.

Changing the parameter for Fairbanks horizontal length, L, changes the magnitude of the model-observation comparison slopes in Table 3, effectively increasing or decreasing the amount of pollution measured near ground level. The value chosen in the "Base" simulation is 4 km, which is the horizontal box edge dimension of the urban area being simulated (Figure 1). Changing the Fairbanks model length, L, does not change the shape of the vertical profile of SO_2, as indicated by the relative insensitivity of the P1/P0 slope ratio to changing L. This shows that the skill of the model in simulating the correct vertical profile of pollution is not sensitive to changes in L; this parameter only affects the amount of pollution trapped in the model. Changing the emissions rates using a multiplier has a similar effect in the model as changing L, where increasing or decreasing the emissions rates increases or decreases both path 0 and path 1 slopes but does not change the P1/P0 slope ratio. Therefore, to the extent that the emissions are not known accurately, the effective horizontal export rate cannot be uniquely determined. However, the ADEC's best estimate of ground level SO_2 emissions, which are only from home heating sources, was used in the downtown areas, and the transport length is realistic with regards to the physical size of downtown Fairbanks, indicating the model performs well with Fairbanks emissions and size.

https://doi.org/10.5194/egusphere-2023-3082
Preprint. Discussion started: 3 January 2024

The constant near-neutral SBL height, $h_{neutral}$ = 400 m used when the atmosphere near the surface is less stable, as indicated by times when $dT_{[23m-3m]} < 0.2$ °C, was also studied. The model was found to be nearly insensitive to $h_{neutral}$. This validates our choice of 400 m for $h_{neutral}$. Although the friction velocity, u*, certainly varies over time, the simulation used a reasonable fixed value, which was perturbed to be $u^* = 0.6$ m s^{-1} or $u^* = 0.25$ m s^{-1} in sensitivity runs Table 3. This perturbation shows that varying the value of u^* had minimal effect on the slopes and R values and that the model results are fairly insensitive to the value of u^*. Overall, the model is mostly sensitive to the SBL height for the vertical shape and to the source (emissions) and sink (affected by Fairbanks length) for the magnitude of pollution at ground level. Periods when the inversion "breaks" are critical for cleaning out pollution and the timing of these events are well predicted by weak temperature inversions and winds penetrating the urban canopy.

5.5 Analysis of modeled steady state transport residence times

The urban canopy column residence time, τ_{canopy}, in the "Base" simulation is typically below an hour, reducing the amount of chemical processing that can occur within the urban canopy, where pollution accumulates to large amounts. While the median column export residence time, τ_{export}, is also relatively short for the downtown Fairbanks area, there are times when this residence time exceeds 5 hours and even approaches 10 hours, suggesting that there may be times when a reservoir of pollution aloft has more time for chemical processing to occur (see Supplement Figure S6). If pollution is transported above the urban canopy layer when the SBL height is taller, it could become trapped in a reservoir aloft if the SBL height then decreases to a shorter altitude. If this "lofted reservoir" of pollution is formed after a decrease in SBL height, then the residence time of pollution in this lofted reservoir will depend upon the horizontal wind speed. If the

https://doi.org/10.5194/egusphere-2023-3082
Preprint. Discussion started: 3 January 2024

horizontal wind speed is large within the lofted reservoir, it will be quickly diluted by background air from outside of Fairbanks and will not downwash processed pollution locally. However, if the horizontal wind speed is slow within the lofted reservoir, there may be time for changes in chemistry to occur within the reservoir and downwash of processed pollution into the urban area could be possible.

6 Conclusion

A version of the PACT-1D model that includes horizontal advection and having vertical dispersion controlled by an eddy diffusivity (K_z) profile based on literature SBL parameterization and driven by a SBL height parameterization based on the near surface temperature inversion strength, was used to simulate SO_2 as a tracer for dispersion. The model was successful in simulating observed in-situ 3 m SO_2 and LP-DOAS path averaged SO_2 from 12 m to 191 m with excellent agreement, with a modeled 3 m versus in-situ 3 m SO_2 correlation coefficient $R = 0.81$ and a model path average versus LP-DOAS path average SO_2 correlation coefficient $R = 0.88$ for all paths.

Idealized steady state simulations validated the model's response to input parameters and yielded vertical profiles and ground level steady state mixing ratios of SO_2 similar to what was measured by LP-DOAS in the field. When the SBL height is shorter, the height of the polluted layer is equivalent to the SBL height, as pollution can vertically mix throughout the shorter SBL height with less horizontal loss by wind, yielding a sigmoid shaped profile. When the SBL height is larger or winds aloft are stronger, winds aloft can dilute pollution that mixes vertically aloft, such that the height of the polluted layer is shorter than the SBL height and the profile is more triangular in shape. The SBL height derived from near-surface temperature difference observations

https://doi.org/10.5194/egusphere-2023-3082
Preprint. Discussion started: 3 January 2024

in downtown Fairbanks ($dT_{[23m-3m]}$) is very shallow when the atmosphere near the ground is stable, never exceeding h = 50 m AGL and becoming as low as h = 20 m AGL for extreme inversion strength. When the atmosphere is near-neutral in the region near ground level (when $dT_{[23m-3m]}$ < 0.2 °C), the model is insensitive to SBL height as long as the SBL height is reasonably large, such as the height used in the model at these times, $h_{neutral}$ = 400 m.

The model successfully captured the vertical profile of SO_2 observations in downtown Fairbanks. When comparing the shortest LP-DOAS path averaged SO_2 mixing ratio versus the in-situ 3 m SO_2 measured at the CTC site, the zero-intercept linear regression analysis had a *slope* = 0.94 and R = 0.89, indicating that pollution is fairly well mixed within a ~15 m urban canopy layer on a three-hour timescale. A series of sensitivity tests were performed to evaluate the model's dependence on input parameters. The model's vertical profile was only sensitive to the SBL height, and generally the surface mixing ratio responded linearly to variations in emissions and the length of Fairbanks, which controls the horizontal exchange rate. The model is fairly insensitive to variations in the neutral BL height and the value of the friction velocity.

The residence time of air in the urban canopy is usually shorter than a few hours, with a median residence time of 40 minutes overall and 54 minutes when stable, and a median column export residence time of 1.8 hours overall and 2.1 hours when stable, limiting time for chemical processing to occur near the ground. Chemical processing may occur within a lofted reservoir of pollution, which can either be removed from the Fairbanks area by horizontal advection, mixed back down into the urban canopy given enough time, or possibly re-circulated back into the urban canopy. However, the model achieves excellent results (R = 0.88) without considering the recycling of pollution or lofted sources such as powerplants, indicating that these effects are not dominant.

https://doi.org/10.5194/egusphere-2023-3082
Preprint. Discussion started: 3 January 2024

Code / data availability

Final data from the study is available on the Arcticdata.io ALPACA data portal (https://arcticdata.io/catalog/portals/ALPACA). From this repository, we include the gas composition, temperature, and wind data from the CTC site, doi:10.18739/A27D2Q87W. The model code and input files will be uploaded to the portal upon acceptance of the manuscript and are provided as a link to reviewers for the purpose of peer review.

Author contribution:

This work was originally authored by M.C.-M. with substantial contributions from W.S. All authors contributed to revisions and editing of the final manuscript. The work is based upon the PACT-1D model, which was developed by J.T. and J.S., and modified for this application by M.C.-M., W.S., J.K., and J.S. Pollution emissions were provided by D.H. and resampled by J.K. Input and validation data was measured and provided by J.S., M.C.-M., S.C., W.S, and T.R. Project conceptualization and funding for the field study was obtained by W.S., J.S., and the ALPACA science team.

Competing interests:

The authors declare that they have no conflict of interest.

Acknowledgements

We thank the entire ALPACA science team of researchers for designing the experiment, acquiring funding, making measurements, and ongoing analysis of the results. The ALPACA

https://doi.org/10.5194/egusphere-2023-3082
Preprint. Discussion started: 3 January 2024

project is organized as a part of the International Global Atmospheric Chemistry (IGAC) project under the Air Pollution in the Arctic: Climate, Environment and Societies (PACES) initiative with support from the International Arctic Science Committee (IASC), the National Science Foundation (NSF), and the National Oceanic and Atmospheric Administration (NOAA). We thank University of Alaska Fairbanks and the Geophysical Institute for logistical support, and we thank Fairbanks for welcoming and engaging with this research. W.R.S. and M.C.-M. acknowledge support from NSF grants NNA-1927750 and AGS-2109134. J.S., J.K., and S.C. acknowledge funding support from NSF grants 1927936 and 2109240. J.L.T. is funded by the European Union's Horizon 2020 research and innovation programme under grant agreement No. 101003826 via project CRiceS (Climate Relevant interactions and feedbacks: the key role of sea ice and Snow in the polar and global climate system). T.R. acknowledges support from the Agence National de Recherche (ANR) CASPA (Climate-relevant Aerosol Sources and Processes in the Arctic) project (grant no. ANR-21-CE01-0017), the Institut polaire français Paul-Émile Victor (IPEV) (grant no. 1215) and Labex Voltaire (grant no. ANR-10-LABX-100-01). We thank Robert Gilliam from the U.S. Environmental Protection Agency for providing the WRF wind speed data. Disclaimer: The views expressed in this article are those of the authors and do not necessarily represent the views or policies of the U.S. Environmental Protection Agency.

References

ADEC: Alaska Department of Environmental Conservation Amendments to: State Air Quality Control Plan, https://dec.alaska.gov/air/anpms/sip/fbks-pm2-5-regs-ammends-2016, 2016.

Ahmed, S., Thomas, J., Tuite, K., Stutz, J., Flocke, F., Orlando, J., Hornbrook, R., Apel, E., Emmons, L., Helmig, D., Boylan, P., Huey, G., Hall, S., Ullmann, K., Cantrell, C., and

https://doi.org/10.5194/egusphere-2023-3082
Preprint. Discussion started: 3 January 2024

Fried, A.: The Role of Snow in Controlling Halogen Chemistry and Boundary Layer Oxidation During Arctic Spring: A 1D Modeling Case Study, Journal of Geophysical Research: Atmospheres, 127, https://doi.org/10.1029/2021JD036140, 2022.

ALPACA: Alaskan Layered Pollution And Chemical Analysis (ALPACA) White Paper, Fairbanks, Alaska, https://alpaca.community.uaf.edu/wp-content/uploads/sites/758/2019/05/ALPACA-whitepaper.pdf, 2018.

Beare, R. J., Macvean, M. K., Holtslag, A. A. M., Cuxart, J., Esau, I., Golaz, J.-C., Jimenez, M. A., Khairoutdinov, M., Kosovic, B., Lewellen, D., Lund, T. S., Lundquist, J. K., Mccabe, A., Moene, A. F., Noh, Y., Raasch, S., and Sullivan, P.: An Intercomparison of Large-Eddy Simulations of the Stable Boundary Layer, Boundary Layer Meteorol, 118, 247–272, https://doi.org/10.1007/s10546-004-2820-6, 2006.

Benson, C. S.: Ice Fog, Eng Sci, 32, 15–19, ISSN 0013-7812, https://resolver.caltech.edu/CaltechES:32.8.ice, 1969.

Bourne, S. M., Bhatt, U. S., Zhang, J., and Thoman, R.: Surface-based temperature inversions in Alaska from a climate perspective, Atmos Res, 95, 353–366, https://doi.org/10.1016/j.atmosres.2009.09.013, 2010.

Bowling, S. A.: Climatology of High-Latitude Air Pollution as Illustrated by Fairbanks and Anchorage, Alaska, Journal of Climate and Applied Meteorology, 25, 22–34, https://doi.org/10.1175/1520-0450(1986)025<0022:COHLAP>2.0.CO;2, 1986.

Bradley, R. S., Keimig, F. T., and Diaz, H. F.: Climatology of surface-based inversions in the North American Arctic, J Geophys Res, 97, 15699, https://doi.org/10.1029/92JD01451, 1992.

https://doi.org/10.5194/egusphere-2023-3082
Preprint. Discussion started: 3 January 2024

733 Brost, R. A. and Wyngaard, J. C.: A Model Study of the Stably Stratified Planetary Boundary
734 Layer, J Atmos Sci, 35, 1427–1440, https://doi.org/10.1175/1520-
735 0469(1978)035<1427:AMSOTS>2.0.CO;2, 1978.
736 Busch, N., Ebel, U., Kraus, H., and Schaller, E.: The structure of the subpolar inversion-capped
737 ABL, Archives for Meteorology, Geophysics, and Bioclimatology Series A, 31, 1–18,
738 https://doi.org/10.1007/BF02257738, 1982.
739 Cesler-Maloney, M., Simpson, W. R., Miles, T., Mao, J., Law, K. S., and Roberts, T. J.:
740 Differences in Ozone and Particulate Matter Between Ground Level and 20 m Aloft are
741 Frequent During Wintertime Surface-Based Temperature Inversions in Fairbanks, Alaska,
742 Journal of Geophysical Research: Atmospheres, 127,
743 https://doi.org/10.1029/2021JD036215, 2022.
744 Degrazia, G. A. and Moraes, O. L. L.: A model for eddy diffusivity in a stable boundary layer,
745 Boundary Layer Meteorol, 58, 205–214, https://doi.org/10.1007/BF02033824, 1992.
746 Geyer, A. and Stutz, J.: Vertical profiles of NO3, N2O5, O3, and NOx in the nocturnal boundary
747 layer: 2. Model studies on the altitude dependence of composition and chemistry, Journal
748 of Geophysical Research D: Atmospheres, 109, https://doi.org/10.1029/2003JD004211,
749 2004.
750 Jacob, D. J.: Introduction to Atmospheric Chemistry, Princeton University Press, 1999.
751 Kotchenruther, R. A.: Source apportionment of PM 2.5 at multiple Northwest U.S. sites: Assessing
752 regional winter wood smoke impacts from residential wood combustion, Atmos Environ,
753 142, 210–219, https://doi.org/10.1016/j.atmosenv.2016.07.048, 2016.
754 Kuhn, M., Lettau, H. H., and Riordan, A. J.: Stability-related wind spiraling in the lowest 32
755 meters, 93–111, https://doi.org/10.1029/AR025p0093, 1977.

https://doi.org/10.5194/egusphere-2023-3082
Preprint. Discussion started: 3 January 2024

Mahrt, L.: Modelling the depth of the stable boundary-layer, Boundary Layer Meteorol, 21, 3–19, https://doi.org/10.1007/BF00119363, 1981.

Mahrt, L.: Intermittent of Atmospheric Turbulence, J Atmos Sci, 46, 79–95, https://doi.org/10.1175/1520-0469(1989)046<0079:IOAT>2.0.CO;2, 1989.

Mayfield, J. A., Fochesatto, G. J., Mayfield, J. A., and Fochesatto, G. J.: The Layered Structure of the Winter Atmospheric Boundary Layer in the Interior of Alaska, J Appl Meteorol Climatol, 52, 953–973, https://doi.org/10.1175/JAMC-D-12-01.1, 201

Monin, A. S. and Obukhov, A. M.: Basic Laws of Turbulent Mixing in the Surface Layer of the Atmosphere, Contrib. Geophys. Inst. Acad. Sci. USSR, 24, 163–187, 1954.

Moon, A., Jongebloed, U., Dingilian, K., Schauer, A., Chan, Y. C., Cesler-Maloney, M., Simpson, W., Weber, R., Tsiang, L., Yazbeck, F., Zhai, S., Wedum, A., Turner, A., Albertin, S., Bekki, S., Savarino, J., Gribanov, K., Pratt, K., Costa, E., Anastasio, C., Sunday, M., Heinlein, L., Mao, J., and Alexander, B.: Primary Sulfate Is the Dominant Source of Particulate Sulfate During Winter in Fairbanks, Alaska, ACS ES&T Air, 2024, https://pubs.acs.org/doi/full/10.1021/acsestair.3c00023.

Nattinger, K. C.: Temporal and spatial trends of fine particulate matter composition in Fairbanks, Alaska, MS, University of Alaska Fairbanks, Fairbanks, 1–144 pp., 2016.

Newsom, R. K. and Banta, R. M.: Shear-Flow Instability in the Stable Nocturnal Boundary Layer as Observed by Doppler Lidar during CASES-99, J Atmos Sci, 60, 16–33, https://doi.org/10.1175/1520-0469(2003)060<0016:SFIITS>2.0.CO;2, 200

Nieuwstadt, F. T. M.: Some aspects of the turbulent stable boundary layer, Boundary Layer Meteorol, 30, 31–55, https://doi.org/10.1007/BF00121948, 1984a.

https://doi.org/10.5194/egusphere-2023-3082
Preprint. Discussion started: 3 January 2024

778 Nieuwstadt, F. T. M.: The Turbulent Structure of the Stable, Nocturnal Boundary Layer, J Atmos
779 Sci, 41, 2202–2216, https://doi.org/10.1175/1520-0469(1984)041, 1984b.
780 Platt, U. and Stutz, J.: Differential Optical Absorption Spectroscopy, Springer Berlin Heidelberg,
781 Berlin, Heidelberg, https://doi.org/10.1007/978-3-540-75776-4, 2008.
782 Schmale, J., Arnold, S. R., Law, K. S., Thorp, T., Anenberg, S., Simpson, W. R., Mao, J., and
783 Pratt, K. A.: Local Arctic air pollution: A neglected but serious problem, Earths Future,
784 https://doi.org/10.1029/2018EF000952, 2018.
785 Shusterman, A. A., Teige, V. E., Turner, A. J., Newman, C., Kim, J., and Cohen, R. C.: The
786 Berkeley Atmospheric CO2 Observation Network: Initial evaluation, Atmos Chem Phys,
787 16, 13449–13463, https://doi.org/10.5194/acp-16-13449-2016, 2016.
788 Simpson, W.R., Mao, J., Fochesatto, G.J., Law, K.S., DeCarlo, P.F., Schmale, J., Pratt, K.A.,
789 Arnold, S.R., Stutz, J., Dibb, J.E., Creamean, J.M., Weber, R.J., Williams, B., Alexander,
790 B., Hu, L., Yokelson, R., Shiraiwa, M., Decesari, S., Anastasio, C., D'Anna, B., Gilliam,
791 R., Nenes, A., St. Clair, J.M., Trost, B., Flynn, J., Savarino, J., Conner, L.D., Kettle, N.,
792 Heeringa, K.M., Albertin, S., Baccarini, A., Barret, B., Battaglia, M.A., Bekki, S., Brado,
793 T.J., Brett, N., Brus, D., Campbell, J.R., Cesler-Maloney, M., Cooperdock, S., Cysneiros
794 de Carvalho, K., Delbarre, H., DeMott, P., Dennehy, C.J.S., Dieudonné, E., Dingilian, K.K,
795 Donateo, A., Doulgeris, K.M., Edwards, K.C., Fahey, K., Fang, T., Guo, F., Heinlein,
796 L.M.D., Holen, A.L., Huff, D., Ijaz, A., Johnson, S., Kapur, S., Ketcherside, D.T., Levin,
797 E., Lill, E., Moon, A., Onishi, T., Pappaccogli, G., Perkins, R., Pohorsky, R., Raut, J-C.,
798 Ravetta, F., Roberts, T., Robinson, E.S., Scoto, F., Selimovic, V., Sunday, M.O., Temime-
799 Roussel, B., Tian, X., Wu, J., Yang, Y.: Overview of the Alaskan Layered Pollution And
800 Chemical Analysis (ALPACA) field experiment, Submitted to ACS ES&T Air, 2023.

https://doi.org/10.5194/egusphere-2023-3082
Preprint. Discussion started: 3 January 2024

801 Stull, R. B.: A heat-flux history length scale for the nocturnal boundary layer., Tellus, Series A,
802 35 A, 219–230, https://doi.org/10.3402/tellusa.v35i11435, 198
803
804 Stutz, J., Alicke, B., Ackermann, R., Geyer, A., White, A., and Williams, E.: Vertical profiles of
805 NO3, N2O5, O3, and NOx in the nocturnal boundary layer: 1. Observations during the
806 Texas Air Quality Study 2000, Journal of Geophysical Research D: Atmospheres, 109,
807 https://doi.org/10.1029/2003JD004209, 2004.
808 Tran, H. N. Q. and Mölders, N.: Investigations on meteorological conditions for elevated PM2.5
809 in Fairbanks, Alaska, Atmos Res, 99, 39–49,
810 https://doi.org/10.1016/j.atmosres.2010.08.028, 2011.
811 Tran, H. N. Q. and Mölders, N.: Numerical investigations on the contribution of point source
812 emissions to the PM2.5 concentrations in Fairbanks, Alaska, Atmos Pollut Res, 3, 199–
813 210, https://doi.org/10.5094/APR.2012.022, 2012.
814 Tsai, C., Wong, C., Hurlock, S., Pikelnaya, O., Mielke, L. H., Osthoff, H. D., Flynn, J. H., Haman,
815 C., Lefer, B., Gilman, J., Gouw, J., and Stutz, J.: Nocturnal loss of NOx during the 2010
816 CalNex-LA study in the Los Angeles Basin, Journal of Geophysical Research:
817 Atmospheres, 119, https://doi.org/10.1002/2014JD022171, 2014.
818 Tuite, K., Thomas, J., Veres, P., Roberts, J., Stevens, P., Griffith, S., Dusanter, S., Flynn, J.,
819 Ahmed, S., Emmons, L., Kim, S., Washenfelder, R., Young, C., Tsai, C., Pikelnaya, O.,
820 and Stutz, J.: Quantifying Nitrous Acid Formation Mechanisms Using Measured Vertical
821 Profiles During the CalNex 2010 Campaign and 1D Column Modeling, Journal of
822 Geophysical Research: Atmospheres, 126, https://doi.org/10.1029/2021JD034689, 2021.

https://doi.org/10.5194/egusphere-2023-3082
Preprint. Discussion started: 3 January 2024

823 Ward, T., Trost, B., Conner, J., Flanagan, J., and Jayanty, R. K. M.: Source Apportionment of
824 PM2.5 in a Subarctic Airshed - Fairbanks, Alaska, Aerosol Air Qual Res,
825 https://doi.org/10.4209/aaqr.2011.11.0208, 2012.
826 Wyngaard, J. C.: Modeling the planetary boundary layer — Extension to the stable case, Boundary
827 Layer Meteorol, 9, 441–460, https://doi.org/10.1007/BF00223393, 1975.
828 Ye, L. and Wang, Y.: Long-Term Air Quality Study in Fairbanks, Alaska: Air Pollutant Temporal
829 Variations, Correlations, and PM2.5 Source Apportionment, Atmosphere (Basel), 11,
830 1203, https://doi.org/10.3390/atmos11111203, 2020.
831 Zhang, Y., Seidel, D. J., Golaz, J.-C., Deser, C., and Tomas, R. A.: Climatological Characteristics
832 of Arctic and Antarctic Surface-Based Inversions, J Clim, 24, 5167–5186,
833 https://doi.org/10.1175/2011JCLI4004.1, 2011.

https://doi.org/10.5194/egusphere-2023-3082
Preprint. Discussion started: 3 January 2024

834 **Tables**

835 **Table 1:** Stable boundary layer height, h, parametrization as a function of near-surface stability.
836 These values are for the "Base" simulation; sensitivity studies vary either the stable ($dT_{[23m-3m]}$ =>
837 0.2 °C or near-neutral ($dT_{[23m-3m]}$ < 0.2°C) boundary layer height.

$dT_{[23m-3m]}$ / °C	h / m
<0.2	400
0.2	50
2	30
5	25
10	20

838

https://doi.org/10.5194/egusphere-2023-3082
Preprint. Discussion started: 3 January 2024

Table 2: Cases 1 through 4 used SBL parameterization (Equation EQ1) to calculate a vertical profile of K_z from a constant SBL height and a linear wind profile, with no wind in an urban canopy from zero to 15 m and a linear increase from 15 m to a constant geostrophic wind above the SBL. A constant SO_2 emissions rate of $6x10^{-9}$ moles m^{-2} s^{-2} was used in each case.

Variable	Case 1	Case 2	Case 3	Case 4
SBL height	h = 25 m	h = 50 m	h = 50 m	h = 100 m
Wind speed	0 m s^{-1} in the first 15 m to a constant 2 m s^{-1} above SBL	0 m s^{-1} in the first 15 m to a constant 2 m s^{-1} above SBL	0 m s^{-1} in the first 15 m to a constant 5 m s^{-1} above SBL	0 m s^{-1} in the first 15 m to a constant 2 m s^{-1} above SBL

https://doi.org/10.5194/egusphere-2023-3082
Preprint. Discussion started: 3 January 2024

Table 3: Results of sensitivity studies for the full ALPACA period. Zero-intercept linear slopes and intercepts are listed for 3-hour path-averaged modeled SO_2 versus LP-DOAS SO_2. The "Base" simulation was set with $u^* = 0.40$ m s^{-1} and $L = 4$ km.

Variation	LP-DOAS R	LP-DOAS slope	3 m in-situ R	3 m in-situ slope	Slope ratio P1/P0
Base	0.88	1.10	0.81	1.28	1.00
$h = ⅔\ h_{base}$	0.87	1.49	0.82	1.87	0.59
$h = 1.5\ h_{base}$	0.86	0.84	0.80	0.91	1.47
$L = ⅔\ L_{base}$	0.88	0.82	0.80	0.99	0.95
$L = 1.5\ L_{base}$	0.87	1.49	0.82	1.67	1.06
$h_{neutral} = ⅔$ base	0.88	1.12	0.81	1.30	1.03
$h_{neutral}$ =1.5 base	0.87	1.09	0.81	1.27	0.99
$u^* = 0.25$ m s^{-1}	0.88	1.19	0.82	1.46	0.92
$u^* = 0.60$ m s^{-1}	0.87	1.04	0.80	1.16	1.07
$E = ⅔\ E_{base}$	0.88	0.75	0.81	0.87	1.02
$E = 1.5\ E_{base}$	0.88	1.64	0.81	1.91	0.99

https://doi.org/10.5194/egusphere-2023-3082
Preprint. Discussion started: 3 January 2024

849 **Figures**

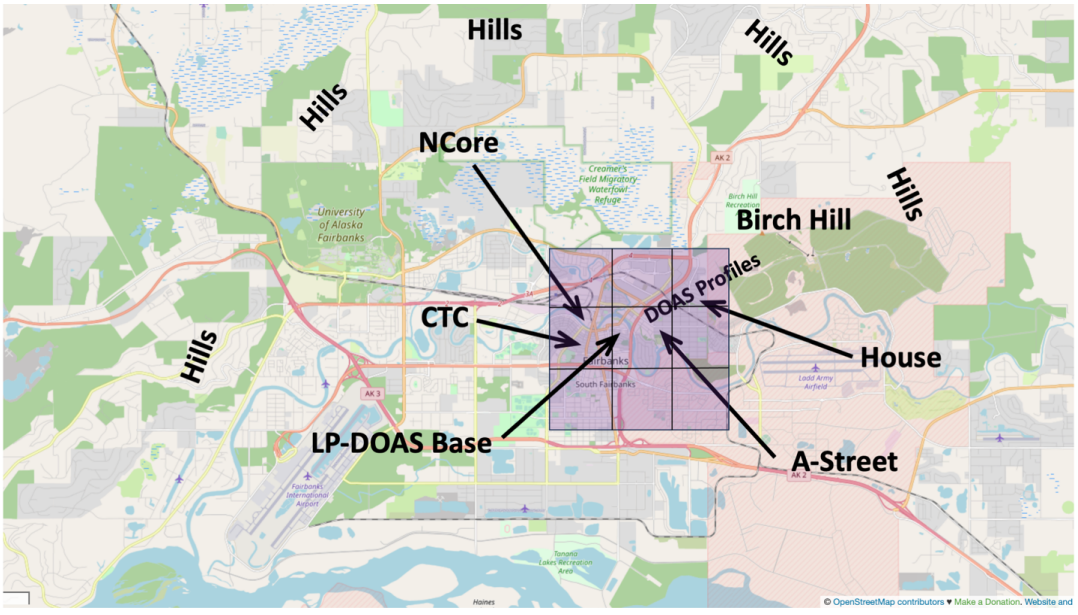

850

851 **Figure 1:** Map of measurement locations in downtown Fairbanks. The purple box represents the
852 area of the nine (3x3) grid cells of the ADEC emissions and WRF-modeled meteorological
853 variables used in PACT-1D. The WRF meteorological variables were taken from the center grid
854 box of the 3x3 grid. Base map was produced by OpenStreetMaps.org using data available under
855 the Open Database License see https://www.openstreetmap.org/copyright.

856

https://doi.org/10.5194/egusphere-2023-3082
Preprint. Discussion started: 3 January 2024

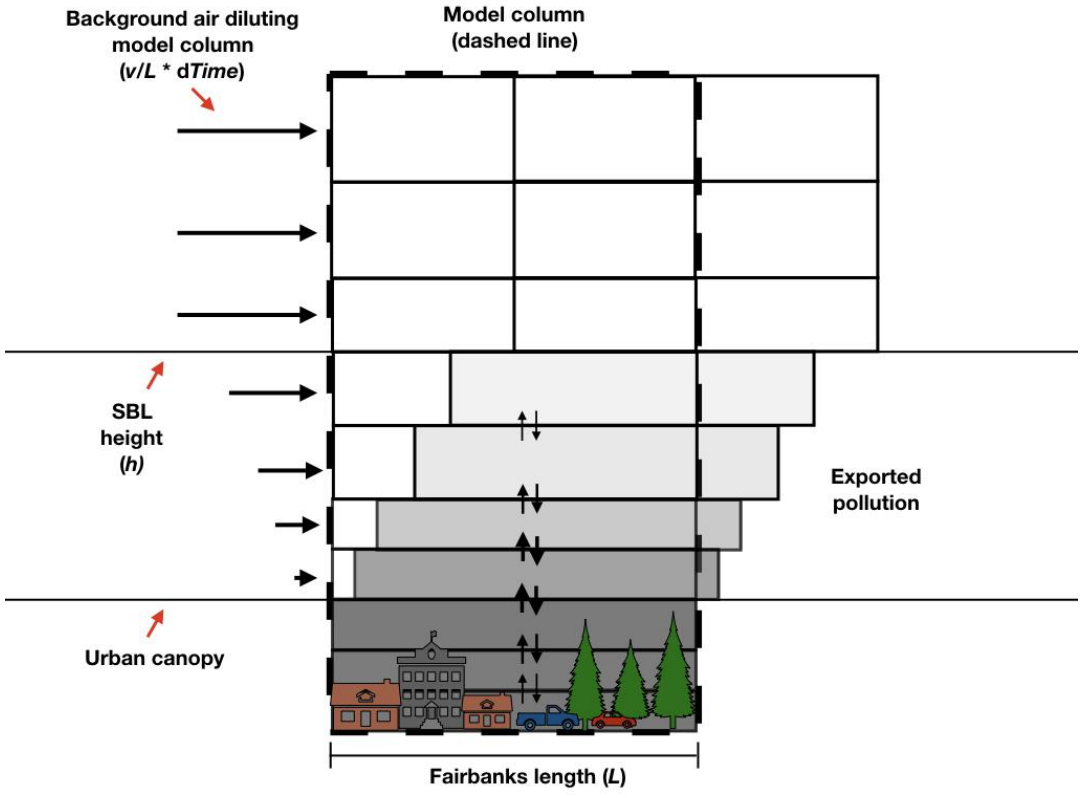

857

858 **Figure 2:** Conceptual model of emissions and dispersion processes used to describe Fairbanks,
859 Alaska within the Platform for Atmospheric Chemistry and Transport one-dimensional model
860 PACT-1D. Emissions occur within the urban canopy where there is no wind to export pollution.
861 Vertical dispersion transports pollution into layers within the SBL where winds bring in clean
862 background air to dilute pollution in the model column and export pollution out of Fairbanks.
863 Vertical dispersion goes to zero both at the ground and at the top of the SBL such that no pollution
864 reaches above the SBL, where there are fast moving, geostrophic winds aloft.

865

https://doi.org/10.5194/egusphere-2023-3082
Preprint. Discussion started: 3 January 2024

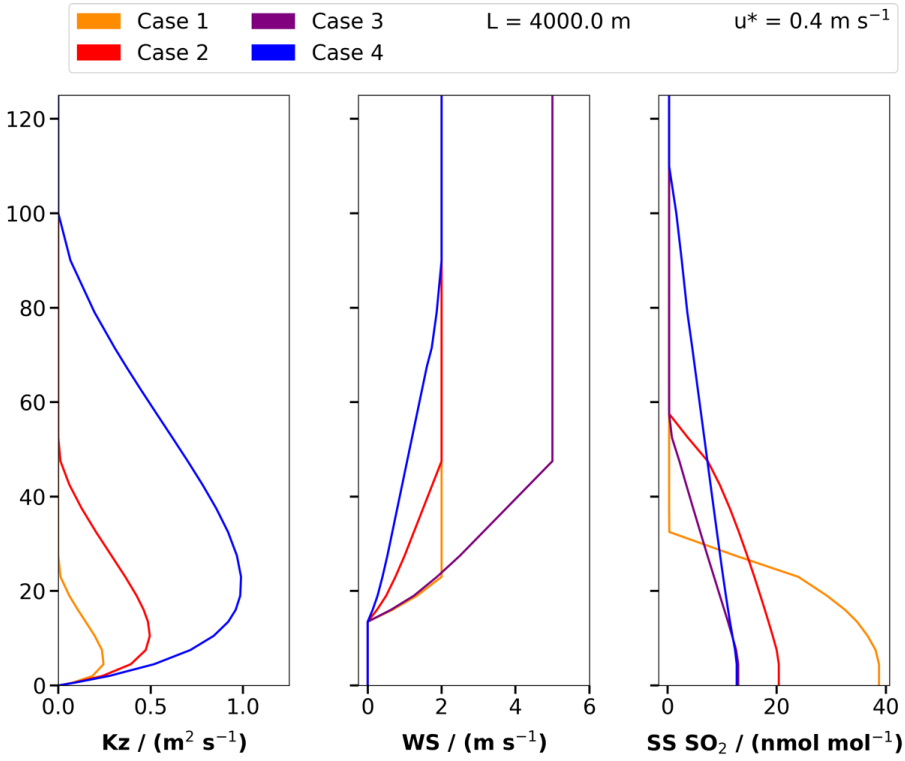

866 **Figure 3:** Vertical profiles of inputs and simulated SO_2 at steady state for various scenarios using
867 downtown column emissions of $6x10^{-9}$ moles m^{-2} s^{-1} SO_2. cases 1 though 4 use the SBL K_z
868 parameterizations from Equation EQ1 with different stable boundary layer heights, h, which are
869 case 1: h = 23 m, cases 2 and 3: h = 50 m, and case 4: h = 100 m. Cases 1 through 4 use a wind
870 model with zero winds in the urban canopy from zero to 15 m AGL, then a linear gradient
871 increasing to achieve a free-atmosphere wind speed at the top of the stable boundary layer. The
872 winds above the SBL are cases 1, 2, and 4: 2 m s^{-1} and case 3: 5 m s^{-1}. The resulting modeled SO_2
873 profiles for each case are also plotted in panel D.
874

https://doi.org/10.5194/egusphere-2023-3082
Preprint. Discussion started: 3 January 2024

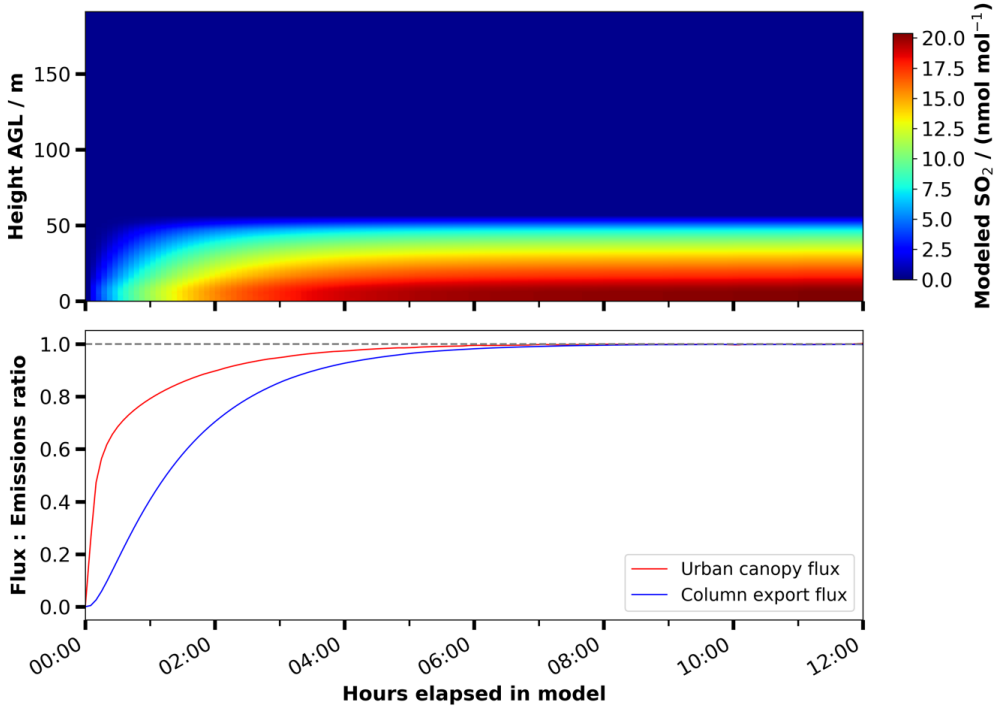

875

876 **Figure 4:** An altitude / time "curtain plot" showing SO_2 mixing ratio represented by colors for the
877 case 2 steady state simulation with a constant 50 m stable boundary layer height. The ratio of the
878 loss rate out of the urban canopy by vertical transport and the export loss rate out of the column
879 by horizontal exchange to the downtown column SO_2 emissions are shown as time series on the
880 bottom panel.

https://doi.org/10.5194/egusphere-2023-3082
Preprint. Discussion started: 3 January 2024

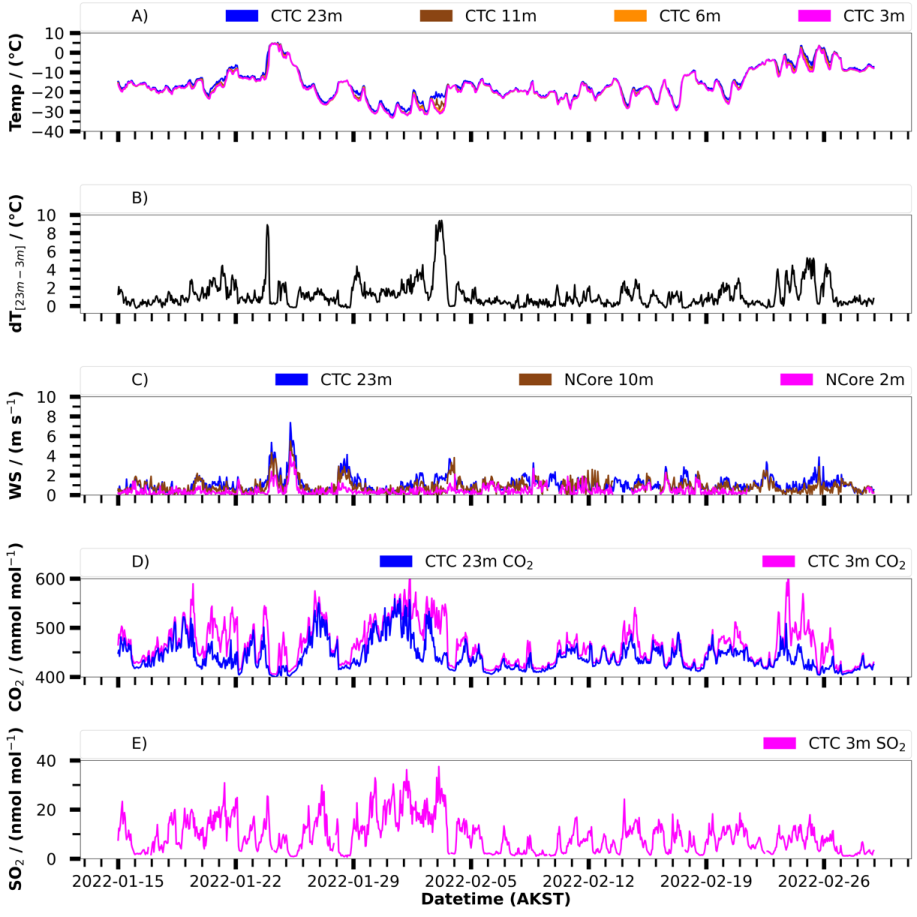

881

882 **Figure 5:** Time series of hourly averaged in-situ field measurements from the UAF CTC site
883 during the ALPACA field campaign in January and February of 2022. The CO_2 in panel D is in
884 micromole mole^{-1} (mmol mol^{-1} is an abbreviation for micromole mole^{-1}).

https://doi.org/10.5194/egusphere-2023-3082
Preprint. Discussion started: 3 January 2024

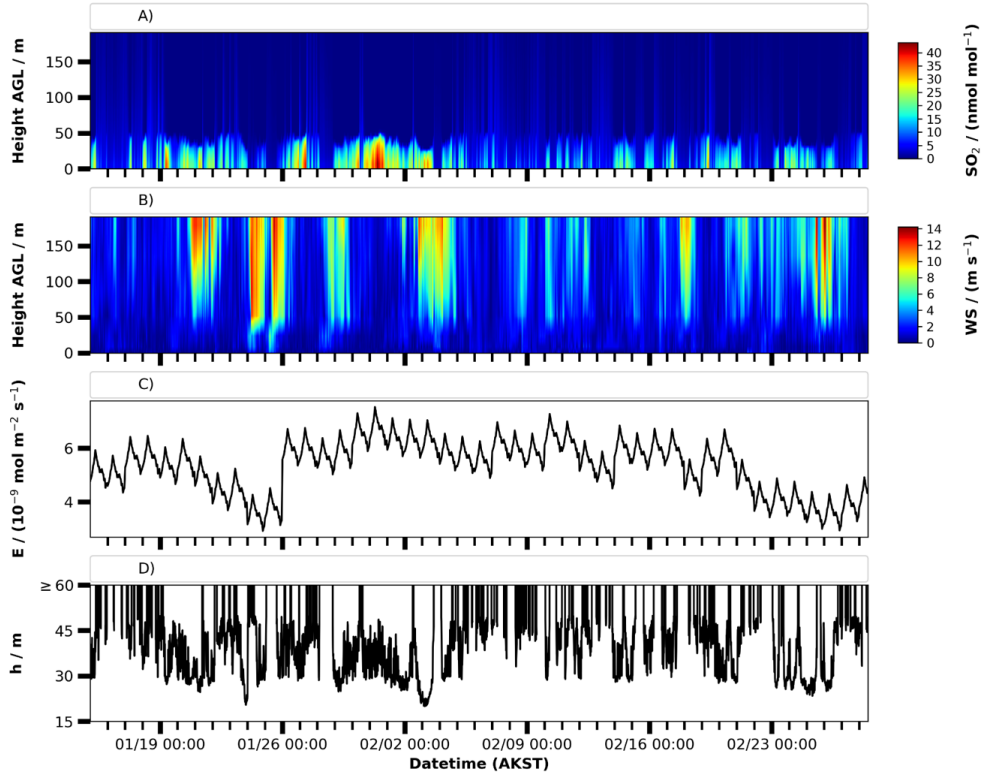

885

886 **Figure 6:** Panels A and B are altitude / time "curtain plots" showing model parameters and results
887 by colors for the ALPACA "Base" simulation. Panel A is modeled SO_2 and panel B is wind
888 speed, *v*. Panel C is a line plot of the SO_2 downtown column emissions rate, *E*, and panel D is a
889 line plot of the stable boundary layer height, *h*. Note that *h* increases off scale to a boundary layer
890 height of 400 m AGL when the atmosphere is near neutral.

https://doi.org/10.5194/egusphere-2023-3082
Preprint. Discussion started: 3 January 2024

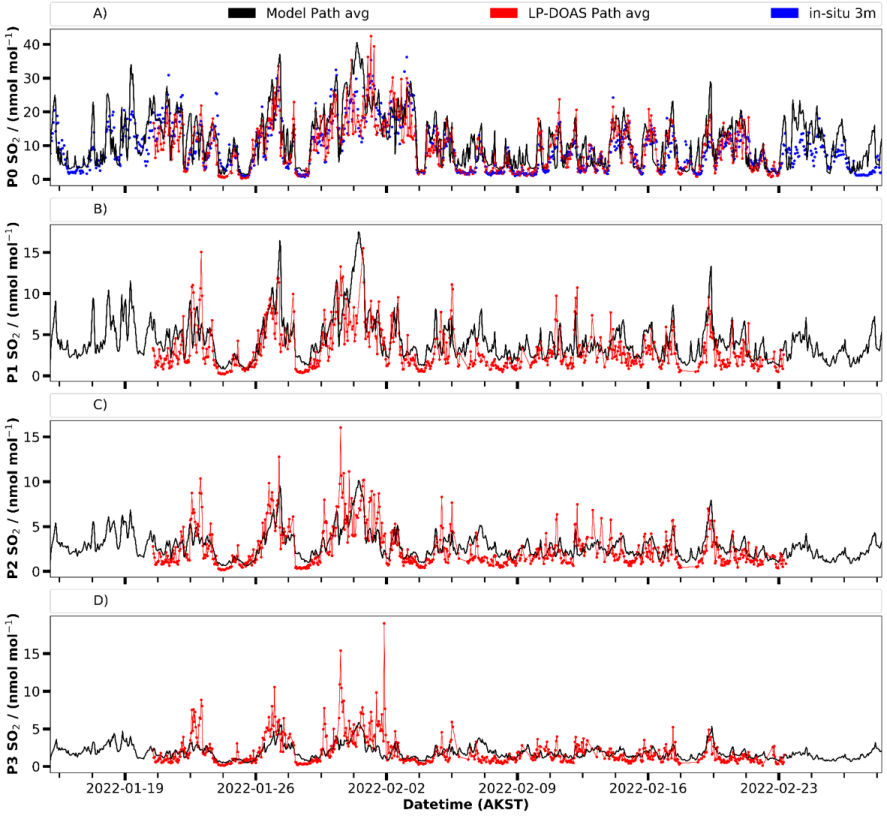

Figure 7: Time series of hourly path-averaged SO_2 from PACT-1D (black line), LP-DOAS field observations (red dots) and in-situ 3 m field observations (blue dots in panel A). Model 3 m data was not included in panel A as the correlation between model 3 m SO_2 and in-situ 3 m SO_2 was good (zero-intercept *slope* = 1.28 and R = 0.81 in Table 1). Panels B through D show the hourly path-averaged LP-DOAS observations and model results for path 1 through path 3, respectively.

https://doi.org/10.5194/egusphere-2023-3082
Preprint. Discussion started: 3 January 2024

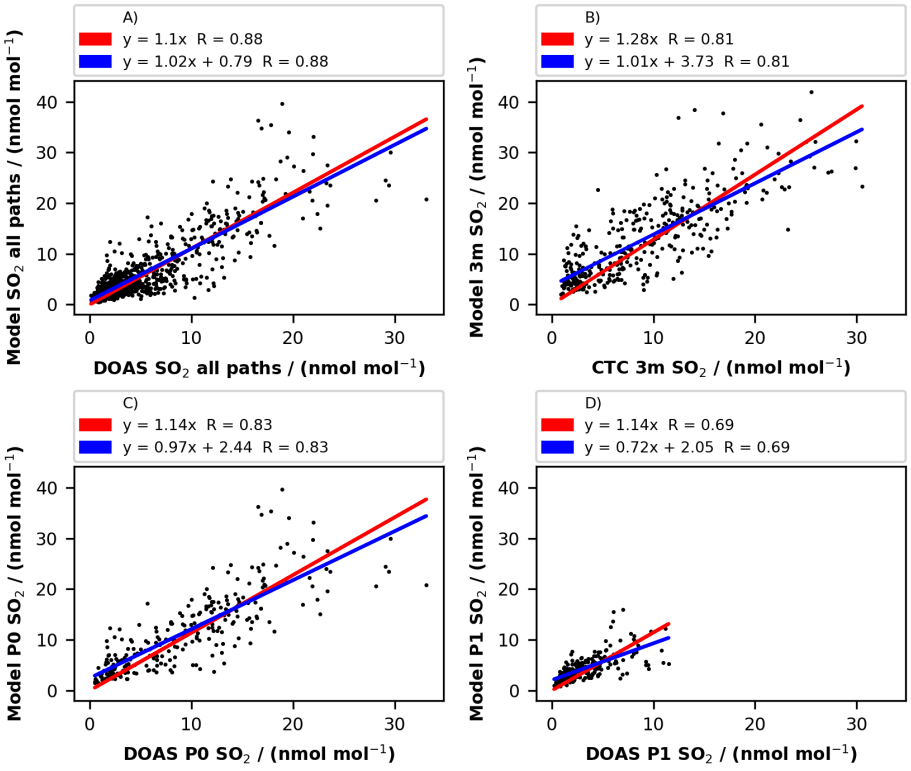

Figure 8: Correlation plots of 3-hour averaged model versus observed SO_2. Panel A shows the model path averaged SO_2 mixing ratio versus the path averaged SO_2 mixing ratio observed by the LP-DOAS for all four DOAS paths from 12 m to 191 m AGL. Panel B shows the modeled SO_2 in the 3 m to 6 m layer in PACT-1D versus the in-situ 3 m SO_2 observed at the CTC site. Panel C shows the model path 0 SO_2 versus the LP-DOAS path 0 SO_2 (path 0 being the average from 12 m to 17 m AGL) and panel D shows the model path 1 SO_2 versus the LP-DOAS path 1 SO_2 (path 1 being the average from 17 m to 73 m AGL). The red lines represent the zero-intercept linear correlation equations and the blue lines represent the free-intercept linear correlation equations, with coefficients for each equation shown in the legend on each panel.

https://doi.org/10.5194/egusphere-2023-3082
Preprint. Discussion started: 3 January 2024

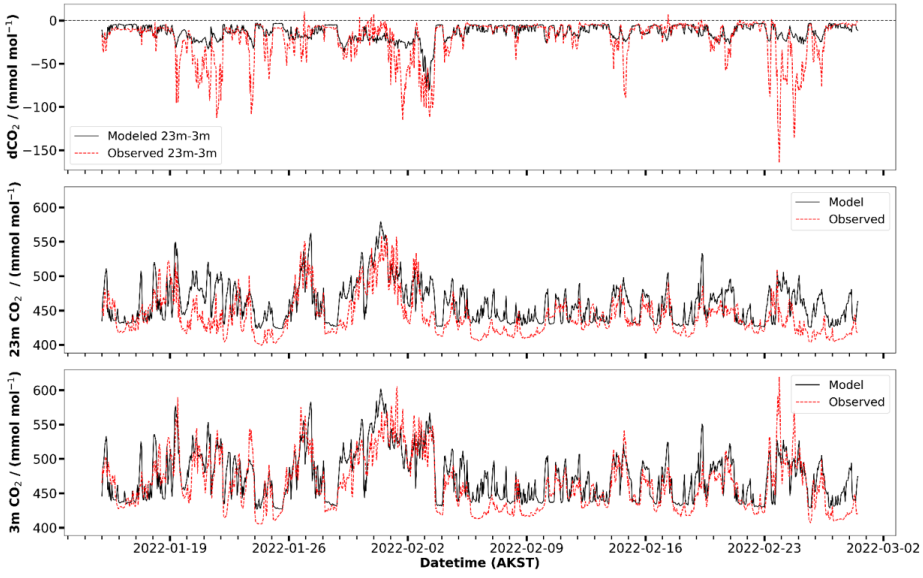

907

908 **Figure 9:** Time series of hourly averaged modeled and in-situ CO_2 measurements at 3 m (bottom
909 panel) and 23 m (middle panel) at the CTC site in downtown Fairbanks. The top panel shows the
910 modeled and observed 23 m minus 3 m CO_2 differences, $dCO_{2[23\ m\text{-}3\ m]}$, in micromole mole^{-1}
911 (mmol mol^{-1} is an abbreviation for micromole mole^{-1}).

912

913

https://doi.org/10.5194/egusphere-2023-3082
Preprint. Discussion started: 3 January 2024

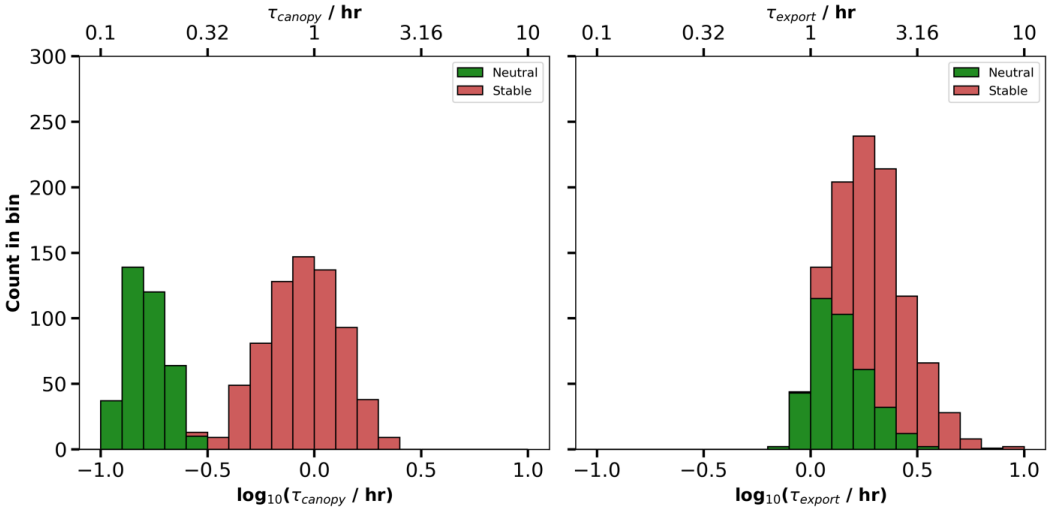

914

915 **Figure 10:** Histograms showing the ALPACA campaign simulated residence time distributions.
916 The left panel shows the steady state urban canopy residence time and the right panel shows the
917 steady-state column export residence time. Note that the histograms are done using logarithmic
918 bins for the residence time on the bottom x-axis and the residence time in hours on the top x-axis.

919

920

https://doi.org/10.5194/egusphere-2023-3082
Preprint. Discussion started: 3 January 2024

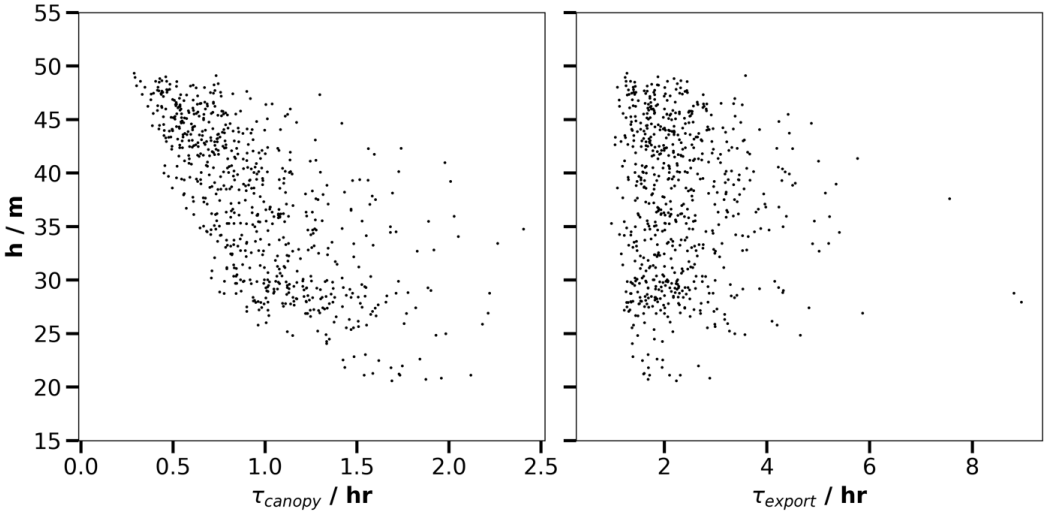

921

922 **Figure 11:** Steady state calculated residence times for the full ALPACA simulation. The left panel
923 shows the urban canopy residence time vs the model stable boundary layer height, *h*, and the right
924 panel shows the column export residence time vs *h*.